

See discussions, stats, and author profiles for this publication at: <https://www.researchgate.net/publication/7944344>

Dual-Luminophore-Doped Silica Nanoparticles for Multiplexed Signaling

ARTICLE *in* NANO LETTERS · FEBRUARY 2005

Impact Factor: 13.59 · DOI: 10.1021/nl048417g · Source: PubMed

CITATIONS

258

READS

68

3 AUTHORS:



[Lin Wang](#)

Merck

28 PUBLICATIONS 2,417 CITATIONS

[SEE PROFILE](#)



[Chaoyong James Yang](#)

Xiamen University

123 PUBLICATIONS 4,605 CITATIONS

[SEE PROFILE](#)



[Weihong Tan](#)

University of Florida

573 PUBLICATIONS 28,474 CITATIONS

[SEE PROFILE](#)

Dual-Luminophore-Doped Silica Nanoparticles for Multiplexed Signaling

Lin Wang, Chaoyong Yang, and Weihong Tan*

Center for Research at Bio/nano Interface, Department of Chemistry and Shands Cancer Center, McKnight Brain Institute, University of Florida, Gainesville, Florida 32611-7200

Received September 26, 2004

ABSTRACT

We have synthesized dual-luminophore-doped silica nanoparticles for multiplexed signaling in bioanalysis. Two luminophores, Tris(2,2'-bipyridyl)osmium(II)bis(hexafluorophosphate) (OsBpy) and Tris(2,2'-bipyridyl)dichlororuthenium(II)hexahydrate (RuBpy), were simultaneously entrapped inside silica nanoparticles at precisely controlled ratios, with desirable sizes and required surface functionality. Single-wavelength excitation with dual emission endows the nanoparticles with optical encoding capability for rapid and high-throughput multiplexed detection. The nanoparticles can be prepared with sizes ranging from a few nanometers to a few hundred nanometers, with specific ratios of luminescence intensities at two well-resolved wavelengths and with excellent reproducibility. These nanoparticles also possess unique properties of high signal amplification, excellent photostability, and easy surface bioconjugation for highly sensitive measurements when used as signaling markers. A simplified ligand binding system using avidin–biotin and an application extension to immunoassays have been explored, demonstrating the potential use of these easily obtainable bioconjugated nanoparticles for multiplexed signaling and bioassays.

Introduction. Development of multiplexed bioassays has recently become an area of rapidly expanding interest and application.^{1–6} Compared to single-target detection methods, multiplexed assays reduce the time and cost per analysis, allow for simpler assay protocols, decrease the sample volumes required, and, most importantly, make comparison of samples feasible and measurements reproducible and reliable. Today's disease diagnosis and biomedical studies all require information from multiple targets such as many proteins and genes for target pattern recognition. Multiplexed assays are thus crucial to complement advances in genomics and proteomics to allow a large number of nucleic acids and proteins to be rapidly screened. Oligonucleotide microarrays^{7–9} and protein arrays^{10–13} can handle a high degree of multiplexed detection using spatially resolved measurements, but the experimental equipment and detection systems are not convenient to use on a routine basis. Lacking real-time monitoring capability, these array technologies cannot be used for biological sample imaging. Multiplexed microsphere-based flow cytometry assays^{14,15} offer several advantages such as flexibility in target selection, fast binding kinetics, and well controlled binding conditions. Both fluorophores and quantum dots have been embedded into polymer microbeads for high-capacity spectral coding.^{5,14,16} With the unique advantage of size-tunable emission and broad excitation properties, quantum dots have the potential

to be an ideal luminophore for wavelength and intensity multiplexing.¹⁶ However, it is not easy to carry out parallel coding on the nanometer scale; many biological systems, including viruses, membranes, and protein complexes, are natural nanostructures. To better understand these structures and to monitor them in real-time, it is becoming increasingly important to develop nanometer scale signaling markers with multiplexed capability.

In this study, we have developed bioconjugated nanoparticles (NPs) for parallel and high-throughput signaling of biomolecules by employing dual-dye based microemulsion processes. We have reported dye-doped silica NPs for a variety of biological/technological applications.^{17–21} Only one type of dye molecules was doped inside silica NPs using a microemulsion method. These NPs have shown unique properties of high signal amplification up to 10 000 times,¹⁹ excellent photostability, and easy surface bioconjugation. Even though many different dye molecules have been used in NP production, the NPs cannot be easily applied to multiplexed analysis with an easy format of single wavelength excitation but multiple wavelength emission to simplify experimental setup and procedures. The problem of single signaling can be solved by using luminescence intensity ratio of two types of dye molecules embedded inside the same NP. Intensity ratios have been effectively used in bioanalysis and bioimaging, providing reproducible measurements and minimizing potential problems such as photobleaching. We have explored this approach by simultaneously

* Corresponding author. E-mail: tan@chem.ufl.edu; (phone and fax) 352-846-2410.

doping two kinds of dye molecules into NPs at precisely controlled ratios with single-wavelength excitation and well-resolved dual emissions. These newly prepared NPs have been tested for multiplexed analysis with flow cytometry, enabling very rapid, highly selective, and sensitive bioassays.

Experimental Section. Reagents. OsBpy [Tris(2,2'-bipyridyl)osmium(II)bis(hexafluorophosphate)] was synthesized according to a previously reported method.²² RuBpy[Tris(2,2'-bipyridyl)dichlororuthenium(II)hexahydrate], TEOS (tetraethyl orthosilicate), APTS [(3-aminopropyl)triethoxysilane], and TX-100 (Triton X-100) were purchased from Aldrich Chemical Co. Inc. (Milwaukee, WI). THPMP [(3-Trihydroxysilyl)propyl methyl-phosphonate] and CTES [carboxyethylsilanetriol, sodium salt] were purchased from Gelest, Inc. (Tullytown, PA). Cyclohexane, *n*-hexanol and ammonium hydroxide (28–30 wt %) were obtained from Fisher Scientific Co. (Pittsburgh, PA). BSA (bovine serum albumin), Tween 20, and MES [2-(*N*-morpholino)ethanesulfonic acid] were obtained from Sigma Chemical Co. (St. Louis, MO). Purified human IgG and mouse IgG, goat antiserum to human serum, and goat antiserum to mouse serum (forensic) were purchased from ICN Pharmaceuticals, Inc. (Aurora, OH). EZ-Link sulfo-NHS-LC-biotin [sulfo-succinimidyl-6-(biotinamido) hexanoate], Sulfo-NHS (*N*-hydroxysulfosuccinimide sodium salt), and EDC [1-ethyl-3-(3-dimethylaminopropyl) carbodiimide hydrochloride] were ordered from Pierce Chemicals (Rockford, IL). Streptavidin-coated microspheres (5.50 μm diameter) and carboxylated silica microspheres (5.06 μm diameter) were ordered from Bangs Laboratories (St. Louis, MO). All other chemicals were of analytical reagent grade. Distilled deionized water (Easy Pure LF) was used for the preparation of all aqueous solutions.

Apparatus. A Hitachi S-4000 scanning electron microscope was used for NP characterization. A Fluorolog TAU-3 spectrofluorometer (Jobin Yvon-Spex, Instruments S. A., Inc., Edison, NJ) was used to record excitation and emission spectra. Optical and luminescence images were obtained by a laser scanning confocal microscope (Olympus, Japan). FACSscan (Becton Dickinson Immunocytometry Systems of San Jose, CA) was used for flow cytometric analysis.

Preparation of Dual-Luminophore-Doped Silica Nanoparticles. RuBpy and OsBpy dyes were prepared in aqueous solutions, respectively, and mixed at precisely controlled molar ratios; the final volumes of the two-luminophore solution mixtures were kept at 480 μL . A water-in-oil microemulsion was prepared by mixing 1.77 mL of TX-100, 7.5 mL of cyclohexane, 1.8 mL of *n*-hexanol, and 480 μL of the dye mixture solutions mentioned above. TEOS (100 μL) was then added as a precursor for silica formation, followed by addition of 60 μL NH_4OH to initiate the polymerization process. The reaction was allowed to continue for 24 h at room temperature, followed by addition of 50 μL of TEOS and either 10 μL of APTS, 40 μL of THPMP (for amine modification), or 50 μL of CTES (for carboxyl modification). The reaction proceeded for another 24 h with stirring. After the reaction was complete, NPs were isolated from the microemulsion using acetone, centrifuged and washed with ethanol and water to remove any surfactant and

dye molecules. Ultrasonication was used during the washing process to remove any physically adsorbed luminophores from the particle surfaces.

Conjugation of Streptavidin Microspheres with Biotinylated Nanoparticles. Biotin-labeled NPs were prepared by reactions between amine-modified NPs and sulfo-NHS-LC-biotin. Streptavidin-coated microspheres were washed by centrifuging three times with phosphate buffer (pH 8.0) containing 0.1% Tween-20 and dissolved in the same buffer to a final concentration of approximately 1.0×10^8 particles/mL. A series of microsphere solutions containing different numbers of particles were prepared and added to an aliquot of excess biotin-NP solutions. The suspension was gently shaken at room temperature for 2 h and analyzed with a Becton Dickinson FACSscan flow cytometer using Ar laser excitation at 488 nm. Orange (585 nm) and red (> 650 nm) luminescence channels were monitored. All solutions passed through the flow cytometer at the same flow rate (60 $\mu\text{L}/\text{min}$) and for the same time period (3 min).

Covalent Coupling of Antibodies to Carboxylated Microspheres and Nanoparticles. Standard procedures²³ were used to crosslink free carboxylic acid groups on NPs with amine-containing antibodies. Briefly, 100 μL of a 0.22% (w/v) suspension of COOH-modified NPs was washed by centrifuging once with deionized water. The pellet was then resuspended in 1 mL of 0.1 M MES, pH 5.5. Aqueous solutions of 10 mM Sulfo-NHS and 4 mM EDC dissolved in MES buffer were prepared, and 0.5 mL of each solution was added to the NP solution. The NPs were incubated at room temperature with gentle agitation. After 15 min, the NPs were centrifuged and washed with 10 mM phosphate buffer, pH 7.4, resuspended in 1.5 mL phosphate buffer, followed by addition of 50 μL of antibodies at a concentration of 1 mg/mL. The mixture was incubated at room temperature for 2 h with gentle end-to-end shaking. NPs were washed in 10 mM phosphate buffer and then resuspended in quenching solution (40 mM Tris-HCl with 0.05 % (w/v) BSA) for 60 min to block free carboxylates. Protein-coated NPs were purified by alternately centrifugating and resuspending in phosphate buffer (10 mM, pH 7.4) with 1% BSA and stored at 4 $^{\circ}\text{C}$ until used. Covalent coupling of secondary antibodies to carboxylated silica microspheres followed the same procedures.

Conjugation of Antibody–Nanoparticles with Secondary-Antibody Microspheres. Antibody-conjugated NPs and secondary-antibody-modified microspheres were diluted in the incubation buffer (10 mM phosphate buffer, pH 7.4, 1% BSA, 0.05% Tween-20), mixed at an experimentally optimized ratio (500:1), and gently shaken at room temperature for 30 min. The resultant product was washed three times by centrifugation (500 rpm, 10 min), resuspended in the same buffer, and stored at 4 $^{\circ}\text{C}$. Luminescence from the NP-coated microspheres was measured with a commercial laser scanning confocal microscope. The Ar ion laser excited at 488 nm wavelength and two orthogonal detection channels, for RuBpy and OsBpy, respectively, were detected with two distinct photomultiplier tubes. Both orange and red channels were saved as 24-bit TIF images.

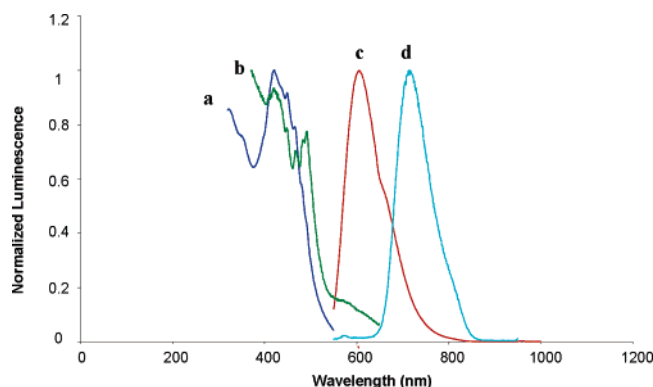


Figure 1. Excitation and emission spectra of RuBpy and OsBpy. (a) Excitation spectrum of RuBpy at 610 nm emission; (b) excitation spectrum of OsBpy at 710 nm emission; (c) emission spectrum of RuBpy at 488 nm excitation; (d) emission spectrum of OsBpy at 488 nm excitation.

Flow Cytometry Experiment for Multiplexed Detection. NPs with luminescence intensity ratios of 9:1 and 2:1 (610:710 nm) were conjugated with human IgG and mouse IgG, respectively. The same number of anti-mouse IgG and anti-human IgG coated microspheres (1.62×10^{-17} mol) were mixed with optimized amounts of mouse IgG and human IgG labeled NPs (8.1×10^{-15} mol). The mixture was diluted with diluent buffer and flown through the flow cytometer.

Results and Discussion. *Dual Dye Nanoparticle Preparation and Characterization.* Figure 1 shows the excitation and emission spectra of RuBpy and OsBpy dyes on a spectrofluorometer. These two dyes share a broad overlapping excitation spectrum but have two distinct maximum emission wavelengths, with RuBpy at 610 nm and OsBpy at 710 nm. By doping these two dyes at certain molar ratios, the NPs provide controllable peak intensity ratios at 610 and 710 nm, upon single wavelength excitation.

NPs were prepared in two steps. During the first 24 h polymerization process, dye-doped silica NPs were formed; the next post-coating procedure allowed various functional groups to be tightly bound to the NPs. The functional groups present on the surface are particularly suitable for coupling reactions with biological molecules. In addition, as each dye-doped NP contains tens of thousands of dye molecules, it exhibits a high signal amplification capability. The luminescence intensity of one dye-doped silica NP is approximately 10^4 times higher than that of one dye molecule. Furthermore, the NPs show excellent photostability. Both RuBpy and OsBpy dyes are transition-metal–ligand complexes (MLCs), they have long lifetimes, and are highly photostable. The double silica coating during the NP preparation process isolates the dye molecules from the outside environment, such as solvent molecules and free radicals caused by light exposure and, therefore, effectively prevent photodecomposition.

The diameter of the carboxyl group modified NPs was 70 ± 3 nm, as characterized by scanning electron microscopy (SEM, Figure 2). The amine modified NPs were of similar size. The functionalized NPs were dispersed very well in aqueous solutions, and no aggregation was observed due to



Figure 2. SEM image of dual-luminophore-doped carboxyl-functionalized NPs.

the electrostatic repulsion force between the NPs. The carboxyl group modified NPs are negatively charged at neutral pH, and the inert phosphonate groups on the amine modified NPs also result in an overall negative surface charge that prevents NP coagulation.

The luminescence intensity ratio of dual dye NPs can be precisely controlled by varying the doping amount of the two dyes. Figure 3a illustrates the emission spectra of several representative NP samples. The inset shows the good correlation between the intensity ratio and the dye molar ratio. To determine whether the intensity ratios have batch-to-batch reproducibility, the average peak intensity ratios from five parallel NP solutions were compared and the coefficient of variation was 7%, indicating that as long as the intensity ratios differ from each other by 14%, the NPs can be fully distinguished in the multiplexed detection.

With this information, a new batch of NP samples without peak ratio overlapping possibility was prepared. Figure 3b shows the normalized emission spectra. The y-axis is the luminescence intensity ratio at 610 nm over that at 710 nm. By controlling the doping concentration of these two dyes, varying intensity ratios ranging from 9:1, 7:1, 5:1, 2:1, 1:1, 1:5, 1:8, 1:17, to 1:27 (488 nm excitation) were obtained, and they all differed from each other by more than 14%. More ratio combinations can be obtained by simply changing the doping amount of the two dyes (RuBpy/OsBpy), making true multiplexed signaling possible and feasible.

Ligand Binding System Using Biotin Nanoparticles and Streptavidin Microspheres. With the newly prepared dual dye NPs, we tested their potential applications in multiple signaling with biotin and avidin as an example. Biotin is a relatively small molecule which has high affinity to avidin and streptavidin ($K_a = 1.3 \times 10^{15} \text{ M}^{-1}$) and has been used widely in bioconjugation for biosensors and bioarrays for genes and proteins.²³ Binding of biotin to avidin is rapid, and once the bond is formed, it is unaffected by most changes such as pH, organic solvents, and other denaturing agents. In this study, biotin-labeled NPs and streptavidin-conjugated

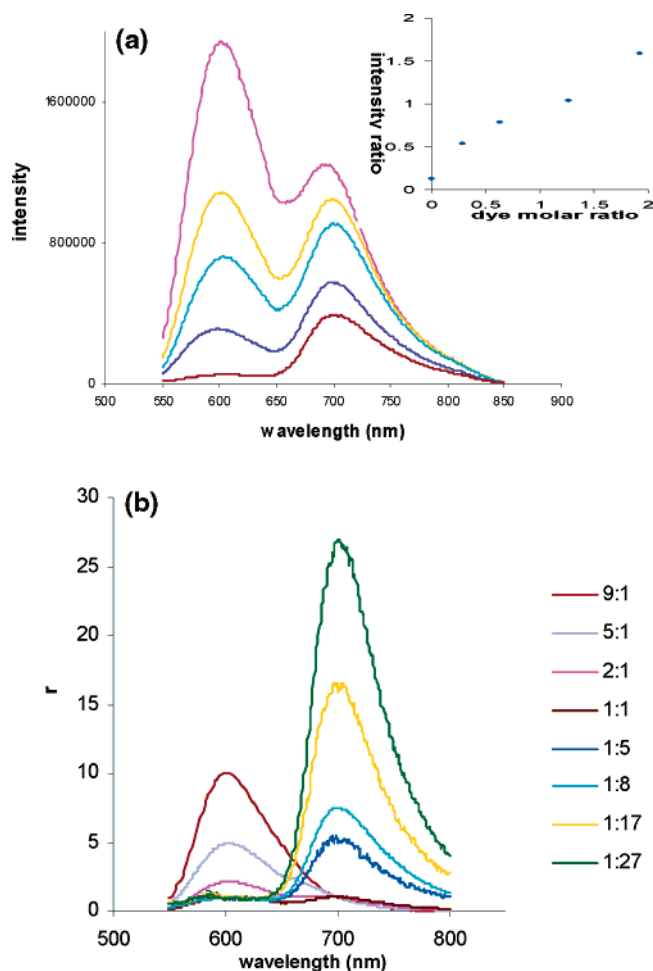


Figure 3. (a) Emission spectra of NPs with varying doping amount of two dyes. Inset: Correlation between the intensity ratio and the molar ratio of the two dyes. (b) Normalized emission spectra of NP samples with different doping concentrations for the two dyes. y-Axis: luminescence intensity ratio at 610 nm to 710 nm. By controlling the doping concentrations of these two dyes, varying ratios ranging from 9:1 to 1:27 (488 nm excitation) were obtained.

microspheres were mixed at an appropriate molar ratio. Avidin–biotin interaction enabled NP assembly on the microsphere surfaces. This assembly was employed initially as a simplified ligand binding system before conducting multiplexed detection.

Amine-modified NPs were reacted with the activated ester of biotin to couple biotin molecules to the NPs. To determine the efficiency of the conjugation, TMR-labeled avidin was mixed with varying quantities of either biotinylated or unbiotinylated NPs. The luminescence intensity of the supernatant solution as a function of the added quantity of NPs was explored and demonstrated the successful biotinylation (data not shown). Streptavidin-coated microspheres were allowed to react with these biotinylated NPs as described in the Experimental Section. The number of NPs that could pack onto the microsphere surfaces was estimated by dividing the theoretical microsphere surface area by the cross-sectional area of a plane bisecting a NP.²⁴ The resulting value was used to determine the minimum number of NPs needed in suspension for each microsphere present. The calculated value was 25 000:1 in this case, and a 50 000:1

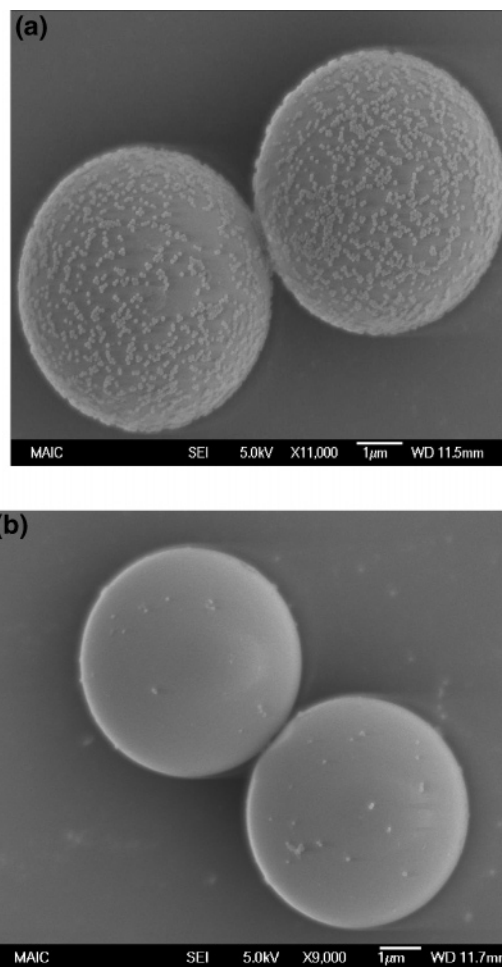


Figure 4. SEM images of streptavidin-coated microspheres with (a) biotinylated NPs and (b) unbiotinylated NPs.

ratio was actually used in the experiment to sufficiently saturate the microsphere surface.

To get a better idea of the microstructure of this composite, scanning electron microscopy of the complex was performed. An SEM image of 70 nm biotin-labeled NPs assembled onto a 5.5 μm diameter streptavidin-coated silica microspheres is shown in Figure 4a. The biotinylated NPs attached to the microspheres, clearly demonstrating binding between biotin and streptavidin. In contrast, there were only minimal NPs on the microsphere surface when the microspheres were treated with nonbiotinylated NPs (Figure 4b).

Flow cytometry experiments were performed using these NP-coated microspheres. Different concentrations of microsphere solutions were mixed with an aliquot of excess biotin-labeled NPs to ensure the successful coating of each microsphere. Bead suspensions were dispersed by vortexing before analysis. The flow cytometer analyzed individual microspheres by size and luminescence. Orange and red luminescence were used for microsphere classification, with the ratio correlating to the peak intensity ratio at 610 and 710 nm measured with the spectrofluorometer. Figure 5 shows the counted events obtained from dot plots as a function of the theoretical concentration of the prepared microsphere solutions. Because each solution passed through the flow cytometer at the same flow rate and for the same

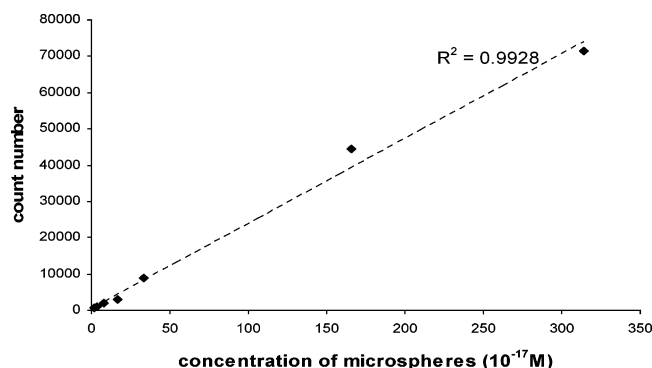


Figure 5. Counted events by dot plots of streptavidin microspheres coated with biotinylated NPs as a function of the theoretical concentration of the microspheres.

time period, the counted number should have a linear relationship with the theoretical concentrations. Figure 5 demonstrates this linear relationship. This model system shows that NPs can be employed successfully for target labeling and counting, and the application extension to multiplexed immunoassays was then performed.

Dual-Luminophore-Doped Silica Nanoparticles for Multiplexed Immunoassays. We designed a model for multiplexed immunoassays using the dual dye NPs. Antibody conjugated NPs with varying intensity ratios and secondary antibody coated microspheres were used for specific immunoassay recognition. The NP/microsphere interaction simulates the recognition process between conjugated NPs and potential receptors/antigens on the surface of a cell or bacterium.

Two individual analytes were used for multiplexed immunoassays. Mouse IgG and human IgG were respectively conjugated to NPs using a carbodiimide-based reaction; goat anti-mouse IgG and goat anti-human IgG were immobilized onto microspheres in a similar way. To verify that the mouse IgG had been successfully conjugated with the NPs, control experiments were performed by adding BSA to replace mouse IgG during the bioconjugation step, followed by addition of TMR-labeled goat anti-mouse IgG. The assembly was centrifuged, and the pellets were dissolved in the phosphate buffer. TMR-labeled goat anti-mouse IgG would specifically bind to mouse IgG conjugated NPs and non-specifically bind to BSA conjugated NPs. The pellets were excited at 545 nm to observe the emission of TMR molecules labeled on the NPs. The substantially higher luminescence intensity from mouse-IgG-coated NPs incubated with TMR-labeled goat anti-mouse IgG verified the successful binding of antibody on the NP surface (data not shown).

Before performing a multiplexed detection, the parameters of each assay need to be optimized separately in a nonmultiplexed format. To do this, individual sets of NPs were conjugated with the target microspheres required for each reaction. After centrifuging and washing, the product was resuspended in buffer solution and mounted on a microscope slide to take images.

As the methods used to control the assembly process involved specific biochemical interactions, it was necessary to verify that the assembled composites were the result of

these specific interactions between the particles and not of nonspecific interactions. Two sets of antibody-coated NPs and two sets of secondary antibody-coated microspheres were cross-reacted following the same procedure mentioned above. To reduce nonspecific binding, incubation buffer contained 1% BSA and 0.05% Tween-20, incubation time was limited to 30 min, and the molar ratio of NPs to microspheres was optimized to achieve the best S/N ratio. The optimized molar ratio of NPs to microspheres was determined to be 500:1. Under these conditions, specific binding between anti-mouse IgG-microspheres with mouse IgG-NPs (Figure 6a) and specific binding between anti-human IgG-microspheres with human IgG-NPs (Figure 6c) were observed, while nonspecific binding between anti-human IgG-microspheres with mouse IgG-NPs (Figure 6b) and nonspecific binding between anti-mouse IgG-microspheres with human IgG-NPs (Figure 6d) were insignificant.

Using these two sets of microspheres, a proof-of-concept flow cytometry experiment was conducted for the detection of mixtures of analytes with dual-luminophore-doped silica NPs. Two kinds of fluorescent NPs were chosen with intensity ratios (610:710 nm) of 9:1 and 2:1, and then labeled with human IgG and mouse IgG, respectively. The same number of anti-mouse IgG and anti-human IgG coated microspheres (1.62×10^{-17} mol, respectively) were mixed with these two kinds of IgG coated NPs (8.1×10^{-15} mol, respectively) to form a cocktail. Figure 7 is a two-dimensional dot plot showing classification of the two microsphere sets based on simultaneous analysis of logarithmic orange luminescence (FL2) and red luminescence (FL3) on a flow cytometer. The dots in the R1 region represent anti-mouse IgG microspheres coated with mouse IgG NPs (2:1 ratio), and those in the R2 region represent anti-human IgG microspheres coated with human IgG NPs (9:1 ratio). The number of dots in the two regions was counted. We expected to have the microspheres equal in these two regions because we used the same number of microspheres. Experimental results show that the population distribution is 46.56% and 53.42%, respectively, in R1 and R2 regions, which correlates well with the expected value when possible binding affinity difference is considered. Thus, we have demonstrated a model for the multiplexed detection of microspheres by bioconjugated NPs. We intend to apply these smart NPs for bacteria/cell recognition, especially those with minimal specific antigens where dye molecules encounter problems. We believe our NPs can bridge this gap due to the following reasons: (1) the higher luminescence intensity of NPs improves the detection limit, especially for some targets which have limited number of surface antigens and (2) the NPs are highly photostable due to the silica matrix protection,^{19–21} while dye molecules suffer from severe photobleaching problem.

The emission peak ratios of the NPs used were 9:1 and 2:1. However, Figure 7 suggests a small overlap in the measurement space that may potentially result in misclassifications of some microspheres from adjacent sets and limit the multiplexed capability. The overlap is due to the collection efficiency of the optical filter configuration

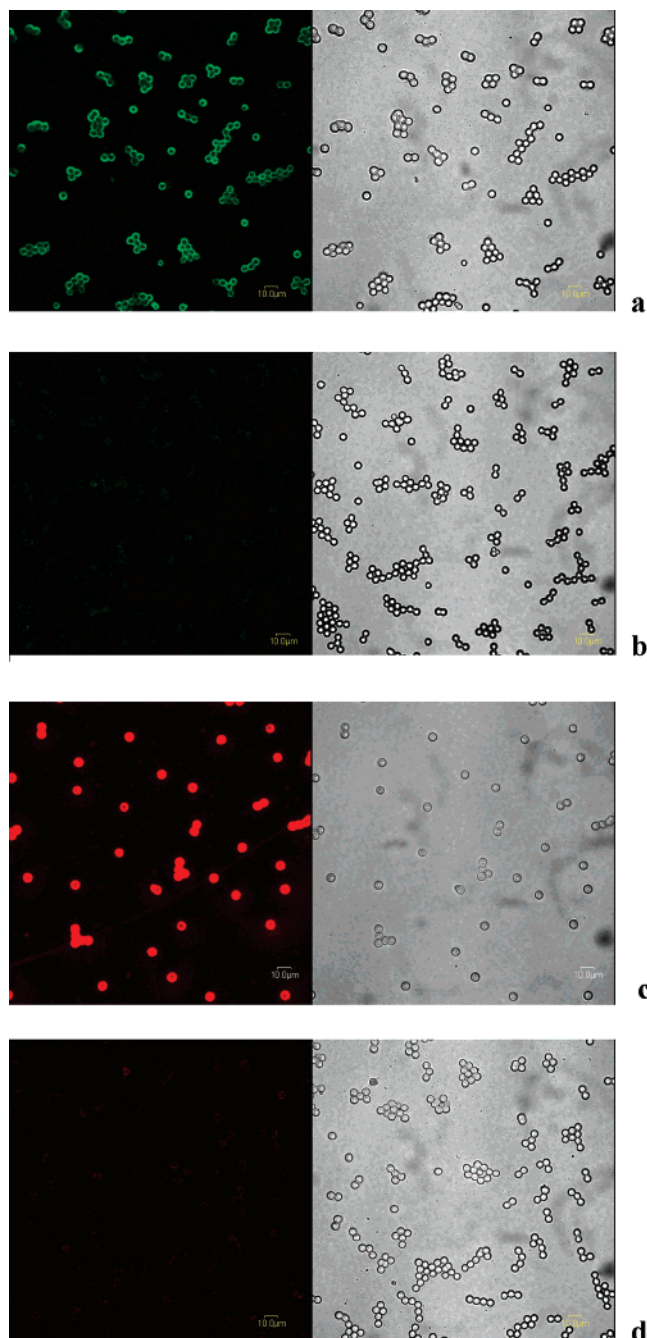


Figure 6. Confocal luminescence images of microspheres coated with NPs under specific or nonspecific reaction conditions: (a) specific binding between anti-mouse IgG conjugated microspheres with mouse IgG conjugated NPs, (b) nonspecific binding between anti-human IgG conjugated microspheres with mouse IgG conjugated NPs, (c) specific binding between anti-human IgG conjugated microspheres with human IgG conjugated NPs, and (d) nonspecific binding between anti-mouse IgG conjugated microspheres with human IgG conjugated NPs.

selected for the flow cytometer measurements. The filters used in the FACScan were band-pass filter (585 ± 42 nm) for orange luminescence channel and long pass filter (> 650 nm) for red luminescence channel, neither of which was optimized for RuBpy or OsBpy dye (the flow cytometer is a multiuser facility and changes of the optical system are not permitted). Multiplexed detection capability could be improved with a more appropriate set of filters.

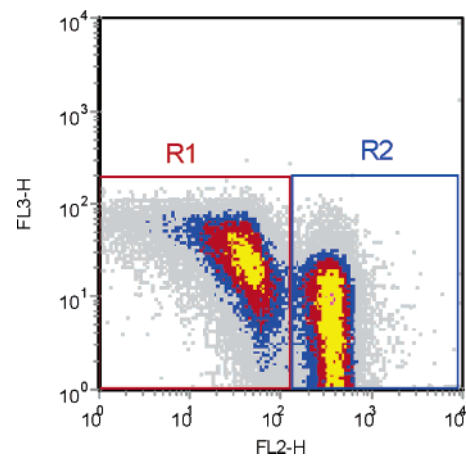


Figure 7. Two-dimensional dot plot showing classification of the two microsphere sets based on simultaneous analysis of logarithmic orange luminescence (FL2) and logarithmic red luminescence (FL3).

Multicolor optical coding using luminescent NPs offers several advantages such as high signal amplification, excellent optical stability, and easy bioconjugation. The multiplexed analysis can be carried out directly at the nanometer dimension level using the newly developed NPs, minimizing artificial interferences. The dye-doped NPs are highly sensitive, which allows detection even at a very low target concentration.¹⁹ The luminescence intensity of one NP is around 10^4 times higher than that of a single dye molecule.^{20,25} This advantage makes NP labeling especially suitable in low target concentration situations. Combined with flow cytometry assays, this method proves to be rapid, selective, and sensitive. In the future, it should offer great flexibility and efficiency in clinical surveillance and detection of infectious diseases, such as rapid diagnosis of multiple bacteria and viruses.

Conclusions. Dual-luminophore-doped silica NPs with different surface modifications have been successfully developed for multiplexed signaling and bioanalysis. These functional NPs can be easily labeled with biomolecules and possess optical encoding capability. By incorporating different amounts of the two luminophores in a single NP, the luminescence intensity ratio can be controlled precisely and made useful for multiple target detection. A model system was used to demonstrate the potential of these NPs for multiplexed bioassays. The procedures are simple and artificial effects are minimal. Furthermore, dye-doped NPs own superior advantages of strong luminescence intensity and excellent photostability, which make these NPs ideal as biolabeling reagents, especially for ultrasensitive detection and under photobleaching-limiting conditions. This method can be used for rapid and sensitive analysis of antigens and nucleic acids, which would have many potential applications in clinical, food, environmental, and forensic laboratories.

Acknowledgment. This work was supported by NIH grants, NSF NIRT grant, and a Packard Foundation Science and Technology award.

References

- (1) Kettman, J. R.; Davies, T.; Chandler, D.; Oliver, K. G.; Fulton, R. J. *Cytometry* **1998**, *33*, 234–243.

- (2) Plowman, T. E.; Durstchi, J. D.; Wang, H. K.; Christensen, D. A.; Herron, J. N.; Reichert, W. M. *Anal. Chem.* **1999**, *71*, 4344–4352.
- (3) Eriksson, S.; Vehniainen, M.; Jansen, T.; Meretoja, V.; Saviranta, P.; Pettersson, K.; Lovgren, T. *Clin. Chem.* **2000**, *46*, 658–666.
- (4) Jani, I. V.; Janossy, G.; Brown, D. W. G.; Mandy, F. *Lancet Infect. Dis.* **2002**, *2*, 243–250.
- (5) Xu, H.; Sha, M. Y.; Wong, E. Y.; Uphoff, J.; Xu, Y.; Treadway, J. A.; Truong, A.; Brien, E. O.; Asquith, S.; Stubbins, M.; Spurr, N. K.; Lai, E. H.; Mahoney, W. *Nucl. Acids Res.* **2003**, *31*(8), e43.
- (6) McBride, M. T.; Gammon, S.; Pitesky, M.; Brien, T. W. O.; Smith, T.; Aldrich, J.; Langlois, R. G.; Colston, B.; Venkateswaran, K. S. *Anal. Chem.* **2003**, *75*, 1924–1930.
- (7) Beaucage, S. L. Strategies in the preparation of DNA oligonucleotide arrays for diagnostic applications. *Curr. Med. Chem.* **2001**, *8*, 1213–1244.
- (8) Stimpson, D. I.; Knepper, S. M.; Shida, M.; Obata, K.; Tajima, H. *Biotechnol. Bioeng.* **2004**, *87*, 99–103.
- (9) Vora, G. J.; Meador, C. E.; Stenger, D. A.; Andreadis, J. D. *Appl. Environ. Microbiol.* **2004**, *70*, 3047–3054.
- (10) Li, Y.; Reichert, W. M. *Langmuir* **2003**, *19*, 1557–1566.
- (11) Peluso, P.; Wilson, D. S.; Do, D.; Tran, H.; Venkatasubbaiah, M.; Quincy, D.; Heidecker, B.; Poindexter, K.; Tolani, N.; Phelan, M.; Witte, K.; Jung, L. S.; Wagner, P.; Nock, S. *Anal. Biochem.* **2003**, *312*, 113–124.
- (12) Qiu, J.; Gurrpide, J. M.; Misek, D. E.; Kuick, R.; Brenner, D. E.; Michailidis, G.; Haab, B. B.; Omenn, G. S.; Hanash, S. *J. Proteome Res.* **2004**, *3*, 261–267.
- (13) Binnun, N. L.; Lindner, A. B.; Zik, O.; Eshhar, Z.; Moses, E. *Anal. Chem.* **2003**, *75*, 1436–1441.
- (14) Spiro, A.; Lowe, M.; Brown, D. *Appl. Environ. Microbiol.* **2000**, *66*, 4258–4265.
- (15) Brodsky, A. S.; Silver, P. A. *Mol. Cell. Proteom.* **2002**, *1*, 922–929.
- (16) Han, M.; Gao, X.; Su, J. Z.; Nie, S. *Nature Biotechnol.* **2001**, *19*, 631–635.
- (17) Santra, S.; Zhang, P.; Wang, K.; Tapeç, R.; Tan, W. *Anal. Chem.* **2001**, *73*, 4988–4993.
- (18) Santra, S.; Wang, K.; Tapeç, R.; Tan, W. *J. Biomed. Optics* **2001**, *6*, 160–166.
- (19) Zhao, X.; Tapeç-Dytioco, R.; Tan, W. *J. Am. Chem. Soc.* **2003**, *125*, 11474–11475.
- (20) Zhao, X.; Bagwe, R. P.; Tan, W. *Adv. Mater.* **2004**, *16*, 173–176.
- (21) Zhao, X.; Hilliard, L.; Mechery, S.; Wang, Y.; Bagwe, R.; Jin, J.; Tan, W. A rapid bioassay for single bacterial cell quantitation using bioconjugated nanoparticles. *Proc. Nat'l. Acad. Sci. U.S.A.* **2004**, *101*, 15027–15032.
- (22) Gauriello, J. G.; Bradley, P. G.; Norton, K. A.; Woodruff, W. H.; Bard, A. J. *Inorg. Chem.* **1984**, *23*, 3–10.
- (23) Hermanson, G. T. *Bioconjugate Techniques*; Academic: San Diego, 1996; pp 176, 591.
- (24) Fleming, M. S.; Mandal, R. K.; Walt, D. R. *Chem. Mater.* **2001**, *13*, 2210–2216.
- (25) Tan, W.; Wang, K.; He, X.; Zhao, X.; Drake, T.; Wang, L.; Bagwe, R. Bionanotechnology based on silica nanoparticles; *Medicinal Research Reviews* **2004**, *24*(5), 621–38.

NL048417G